

An Ultraclean Tip-Wear Reduction Scheme for Ultrahigh Density Scanning Probe-Based Data Storage

Noureddine Tayebi,^{†,*} Yuegang Zhang,^{†,§,*} Robert J. Chen,[†] Quan Tran,[†] Rong Chen,[†] Yoshio Nishi,[‡] Qing Ma,[†] and Valluri Rao[†]

[†]Intel Corporation, 2200 Mission College Boulevard, Santa Clara, California 95054, United States, [‡]Department of Electrical Engineering, Stanford University, 420 Via Palou Mall, Stanford, California 94305, United States, and [§]The Molecular Foundry, Lawrence Berkeley National Laboratory, Berkeley, California 94720, United States

The probe-based seek-and-scan data storage system is an ideal candidate for future ultrahigh-density (>Tbit/inch²) nonvolatile memory devices.^{1–8} In such a system, an atomic force microscope (AFM) probe (or an array of AFM probes) is used to write and read data on a nonvolatile medium. While various writing mechanisms^{1–8} have been proposed for probe-based storage, a great deal of attention has recently been devoted to the pulse writing on ferroelectric films due to the nondestructive nature of the write–erase mechanism.^{1–5} When a short electrical pulse is applied through a conductive probe on a ferroelectric film, the highly concentrated electric field can invert the polarization of a local film volume, resulting in a nonvolatile ferroelectric domain that is the basis of data recording. This mechanism allows for longer medium lifetime, *i.e.*, larger number of write–erase cycles that are comparable to hard disk drives, faster write and read times,⁹ smaller bit size,⁵ and higher storage densities.⁵ High data access rate, however, requires a sliding velocity on the order of 5–10 mm/s, over a lifetime of 5–10 years, corresponding to probe tip sliding distances of 5–10 km. The bit size, and thus the storage density, mainly depends on the radius of the probe tip, which is prone to rapid mechanical wear and dulling due to the high-speed contact mode operation of the system.^{5,10–12} This tip wear can cause serious degradation of the write–read resolution over the device lifetime.

In principle, the tip wear rate could be reduced by using hard conductive diamond coatings.⁵ However, such coatings are usually deposited at high temperatures (~900 °C), which are not compatible with

ABSTRACT Probe-based memory devices using ferroelectric media have the potential to achieve ultrahigh data-storage densities under high write–read speeds. However, the high-speed scanning operations over a device lifetime of 5–10 years, which corresponds to a probe tip sliding distance of 5–10 km, can cause the probe tip to mechanically wear, critically affecting its write–read resolution. Here, we show that the long distance tip-wear endurance issue can be resolved by introducing a thin water layer at the tip–media interface—thin enough to form a liquid crystal. By modulating the force at the tip–surface contact, this water crystal layer can act as a viscoelastic material which reduces the stress level on atomic bonds taking part in the wear process. Under our optimized environment, a platinum–iridium probe tip can retain its write–read resolution over 5 km of sliding at a 5 mm/s velocity on a smooth ferroelectric film. We also demonstrate a 3.6 Tbit/inch² storage density over a 1 × 1 μm² area, which is the highest density ever written on ferroelectric films over such a large area.

KEYWORDS: nanotribology · wear · probe-based storage · ferroelectric media.

integration processes of on-chip electronic circuits.² The diamond coatings are also very rough and have to be sharpened by focus ion beam schemes to reduce the tip radius in order to achieve the required write–read resolution,⁵ which makes it difficult for large-scale batch fabrication of probe arrays.^{2,10} Carbon nanotube probe tips, which due to their cylindrical shape can retain their write–read resolution even after significant wear, have also been proposed.^{13,14} It will, however, take a significant time and research effort to bring the nanotube probes to large-scale fabrication.^{2,10} Thus conventional conductive coatings with a small tip radius that can be deposited at ambient or low-temperature conditions, such as platinum–iridium (PtIr), remain the best choice at the present time.

However, PtIr coatings possess a hardness H and an elastic modulus E comparable to those of the Pb(Zr_{1–x}Ti_x)O₃ (PZT) ferroelectric films used in this study and are hence prone to severe mechanical wear under high sliding speeds on PZT films over

*Address correspondence to yzhang5@lbl.gov.

Received for review June 15, 2010 and accepted September 24, 2010.

Published online October 7, 2010. 10.1021/nn1013512

© 2010 American Chemical Society

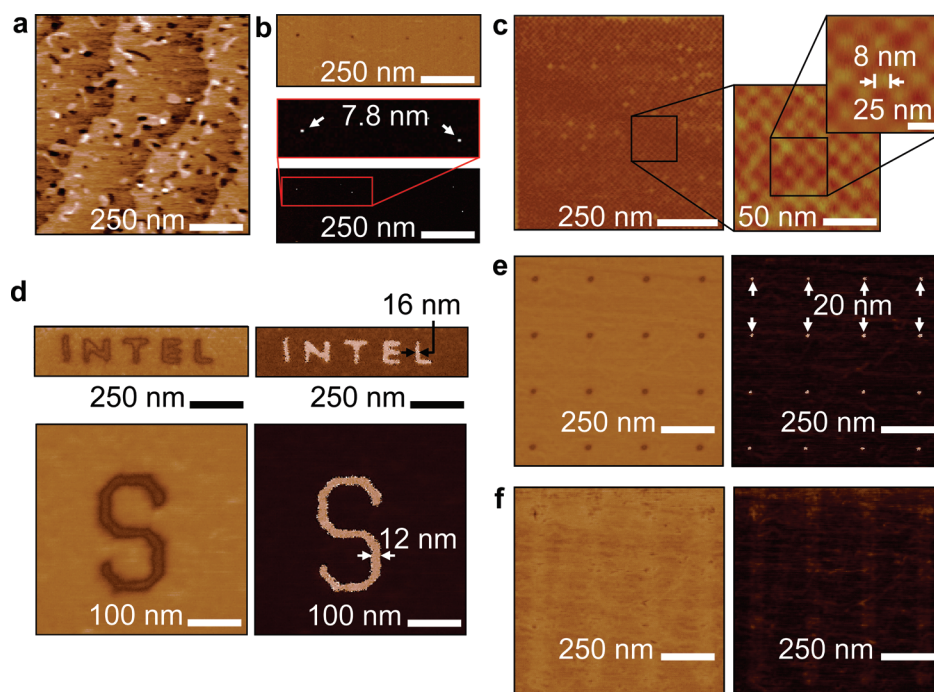


Figure 1. Ultrahigh density storage using probe-based nonvolatile memory devices. (a) Topographical height image of an atomically smooth PZT film with a 0.20 nm rms roughness used as a storage medium. (b) PFM amplitude (top) and phase (bottom) images of the PZT film surface with a 4×1 matrix of 7.8 nm ferroelectric inverted domains formed by applying 100 μs pulses of 3 V to the film through Ptlr probe tips. (c) 3.6 Tbit/inch² ultrahigh density storage density over a $1 \times 1 \mu\text{m}^2$ area (see Supporting Information for procedure). (d) Ferroelectric domain patterns with sub 20 nm resolution written by applying a series of 5 V pulses. (e) Amplitude and phase images of a 4×4 matrix of 20 nm ferroelectric inverted domains written at 5 V pulses. (f) Amplitude and phase images of the same area after erasing the inverted domains by applying -5 V pulses.

short (~ 300 m) distances, as recently reported.¹¹ As determined by the nanoindentation technique, $H_{\text{Ptlr}} = 7$ and $E_{\text{Ptlr}} = 190$ GPa, whereas $H_{\text{PZT}} = 8$ and $E_{\text{PZT}} = 123$ GPa. Wear reduction through conventional lubrication cannot be used either because most common lubricants are organic, which can induce carbonaceous contamination build up on the probe tip during sliding and hinder the pulse writing process (see Supporting Information). An alternative wear reduction mechanism is therefore required.

In this study, we demonstrate a wear endurance mechanism which allows a conductive Ptlr-coated probe tip sliding over a ferroelectric film at a 5 mm/s velocity to retain its write–read resolution over a 5 km sliding distance. This is achieved by sliding the probe tip at a low applied force on atomically smooth PZT surfaces and by modulating the force in the presence of a thin water layer—thin enough not to form a meniscus at the tip–medium interface. Under the force modulation mode, this layer acts as a viscoelastic film, which greatly reduces friction and wear. We also demonstrate storage densities of 3.6 Tbit/inch² over a $1 \times 1 \mu\text{m}^2$ area, which are enabled by the atomically smooth PZT surfaces. This is, to our knowledge, the highest density ever written on ferroelectric films over such a large area. The demonstrated wear endurance mechanism can also be applied to other scanning probe-based systems, such as AFM-based lithography.^{15,16}

RESULTS AND DISCUSSION

Ultra-High Density Writing on Atomically Smooth Thin

Ferroelectric Films. Figure 1a shows a topographic AFM image of a typical PZT ferroelectric film used in the current study. These single crystal PZT films are grown on single crystal SrRuO₃/SrTiO₃(100) substrates using metal–organic chemical vapor deposition (MOCVD)¹⁷ (see Methods Section). The roughness of these films is controlled by varying the Pb precursor flux¹⁷ (see Methods Section). Atomically smooth films with a root-mean-square (rms) roughness down to 0.17 nm have been achieved with this method (Figure 1a). The PZT films are initially polarized in an upward direction and placed on a grounded electrode. A matrix of downward polarization domains is written by applying a series of short positively biased pulses to the PZT surface through a Ptlr conductive probe.

Figure 1b shows piezoresponse force microscopy (PFM) amplitude and phase images of a 3×1 matrix depicting 7.8 nm inverted domains written by applying 100 μs wide pulses of 3 V (see Methods Section). Such single-digit nanometer domains can be written in a checkerboard configuration to achieve ultrahigh density storage. Figure 1c shows $1 \times 1 \mu\text{m}^2$ with a 3.6 Tbit/inch² density (see Supporting Information for procedure). This density is enabled by the atomic smoothness of the PZT surface, which allows for highly localized electric fields to be generated underneath the probe

tip under shorter pulses. This leads to bit scaling down to single nanometer digits (see Supporting Information). The writing defects seen in Figure 1c are due to electrical hot spots originating from defects in the ferroelectric film and not due to the writing scheme, which includes a dual complementary metal-oxide semiconductor (CMOS) switching mechanism. In these regions, the electric field is smaller than other areas where recording was obtained, which causes bits to not be written. These hot spots with a resistance in the range of 590 k Ω –120 M Ω correspond to dead spots during the PFM readout (see Supporting Information). Since those defects are permanent dead bits, they can be mapped out by the storage devices during the media-formatting operation and excluded from the data storage operation. After excluding the observed defect density in our samples, the storage density will still be over 3.3 Tbit/inch². This is, to our knowledge, the highest storage density ever achieved over such a large area. A 10 Tbit/inch² density has previously been reported by Cho *et al.*⁵ but over an area of 50 \times 40 nm only. We also estimate the signal-to-noise ratio (SNR) from our data to be above 10 dB in most areas. More complex patterns with line widths close to 10 nm can also be written, as shown in Figure 1d. Inverted domains can also be easily erased by applying short pulses of the same width but of a reverse polarity (Figure 1e and f) or simply be overwritten.

5 km Tip Wear Endurance Mechanism. For practical data storage applications, the operations shown in Figure 1 have to be achieved at high access rates with sliding velocities on the order of 5–10 mm/s, over a lifetime of 5–10 years, corresponding to sliding distances of 5–10 km. Over such prolonged periods of contact with the film, the conductive probe tip will mechanically wear off, which will degrade the write, read, and erase resolutions of the storage device. The endurance of the device is therefore completely determined by probe tip wear given that ferroelectric media possess very high write–erase endurance cycles. This is different from how endurance is measured in other technologies where only the medium longevity is taken into account. If the area A scanned by the probe tip writing at a bit pitch t , the effective number of endurance cycles is then defined as $(T \times t)/A$, where T is the maximum distance traveled by the probe tip beyond which data read/write becomes unreliable. For example if $T = 5$ km, $t = 15$ nm, and $A = 50 \times 50 \mu\text{m}$, the number of endurance cycles is equal to 6×10^4 . Since a ferroelectric medium can be directly overwritten, all these cycles would be available for data read/write, and a large value of T leads to high endurance.

To obtain such probe tip endurance, various mechanical wear regimes have to be understood. These include stick–slip, abrasive, adhesive, and fatigue wear.¹⁸ The stick–slip regime usually occurs at low speeds¹⁹ and is therefore not relevant for the current study. Abra-

sive wear occurs when the probe tip slides over a rough surface, which can cause local plastic deformation and fracture during tip-asperity contact even at the lightest loads.¹⁸ It can thus be reduced by using atomically smooth surfaces. Adhesive wear is the result of adhesion or bonding that occurs when the probe tip, which is sheared by sliding, is in contact with the surface and can occur regardless of lubrication.¹⁸ This is the dominant mechanism when atomically smooth surfaces are used. Finally, the fatigue wear mechanism occurs during repeated contact cycles between the probe tip and the surface which can result in surface cracks that can cause large debris and fragments to be removed.¹⁸ As seen subsequently, this mechanism is not observed in the current study.

The adhesive wear is described by the well-known Archard's wear model where the wear volume V is proportional to the applied normal force F_N , and the sliding distance x , *i.e.*, $V = CF_N x$, where C is a constant.¹⁸ The constant C depends on the nature of contact. In plastic contact, $C = k/H$, where H is the hardness of the material, and k is a nondimensional wear coefficient that depends on the materials in contact, the surface contamination, and the lubricant used.¹⁸ In elastic contact, $C = k/(E^*(\sigma/R)^{1/2})$, where E^* is the composite elastic modulus between the Ptlr coating and the PZT films, which is defined as $1/E^* = (1 - \nu_{\text{Ptlr}}^2)/E_{\text{Ptlr}} + (1 - \nu_{\text{PZT}}^2)/E_{\text{PZT}}$. Here ν_{Ptlr} (PZT) and E_{Ptlr} (PZT) are the Poisson's ratio and elastic modulus of Ptlr (PZT). While σ is the standard deviation of surface heights, which can be approximated by the rms roughness, and R is the composite mean radius of curvature of the tip–surface system defined as $1/R = 1/R_{\text{Ptlr}} + 1/R_{\text{PZT}}$. Under sliding, the transition from elastic to plastic adhesive wear regimes occurs when the mean flow pressure p_m reaches the value $H/(1 + 9\mu^2)^{1/2}$, where μ is the friction coefficient.¹⁸

Note that in the elastic adhesive wear regime, the wear volume is inversely proportional to the elastic modulus, whereas it is inversely proportional to the hardness in the case of the plastic adhesive wear regime. Given that the elastic modulus of materials used here, *i.e.*, Ptlr and PZT, is two orders of magnitude higher than the hardness, one can reduce the wear volume by two orders of magnitude by operating in the elastic adhesive wear regime. Therefore, we should ideally operate the system at low loads using ultrasoft surfaces. Under such conditions, the effects of the plastic adhesive and abrasive wear mechanisms are greatly reduced, leaving the dominant wear mechanism to be the elastic adhesive wear which, however, could still be significant enough to cause write–read resolution degradation under a constant force load, as shown subsequently.

Modulating the normal force F_N exerted by the probe tip on the surface at ultrasonic frequencies^{20,21} or at cantilever resonance frequency by electrostatic actuation^{19,22,23} has previously been shown to signifi-

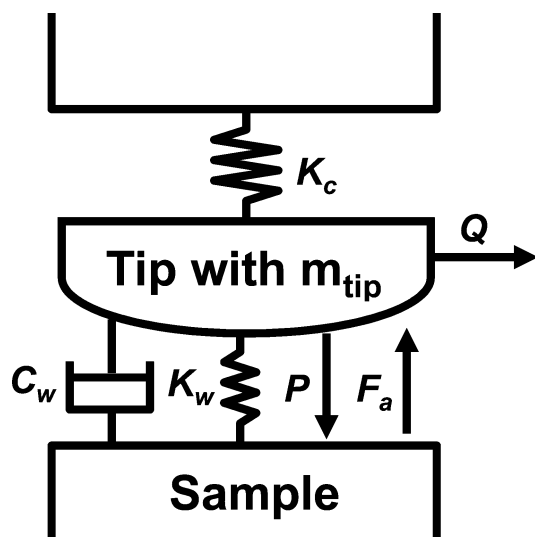


Figure 2. Suggested dynamic contact model during sliding under force modulation in the presence of a thin water film; k_c , m_{tip} , c_w , k_w , P , Q , and F_a are the cantilever spring, tip mass, water layer damping coefficient, water layer spring, contact load, tangential force, and adhesion force, respectively. The equation of motion and friction coefficient for this model are $m_{\text{tip}}\ddot{z} + c_w\dot{z} + (k_c - k_w)z - P(t) + m_{\text{tip}}g + F_a(t) + F_N(1 + \alpha \cos(\omega t)) = 0$ and $\mu = Q/P(t) + k_1z - F_a(t) - cz$.

cantly reduce friction at low sliding speeds and applied forces under both ambient and ultrahigh vacuum conditions. Such observations suggest that the reduced friction is due to lower wear rates which can significantly reduce the friction dissipation energy.²⁴ Previous studies have shown that tip wear occurs through an atom-by-atom loss process without any sudden fracture.¹² We believe that if the elastic adhesive wear is dominant, the force modulation will allow the probe tip to recover elastically during sliding every time the nominal force is reduced during a modulation cycle. This would relax the stress level on bonds between atoms that are taking part in the wear process, delay bond breaking, and thus reduce wear. In addition, the change in contact area with normal force has been shown to follow a sublinear relationship (two-thirds power law).²⁵ Therefore the number of atoms taking part in the wear process also changes during a modulating cycle.

Moreover, the insertion of an ultrathin water film that is a few monolayers in thickness at the tip–sample interface can also provide further wear rate reduction. Such a thin film strongly adheres to the surface, thus forming a liquid crystal, and is not energetically favored to form a meniscus at the tip–sample interface.²⁶ Under force modulation of high frequency, this water film can act as a viscoelastic material, which would further reduce the stress level on such bonds and decrease friction and wear. Figure 2 shows the dynamic contact model at the tip–sample interface under force modulation and in the presence of the ultrathin water layer. Moreover, water is carbon free and of high dielectric

constant, which is ideal as a clean lubricant for our system. The high dielectric constant $\epsilon_r \cong 80$ of the water film has also the advantage of enhancing the tip–sample electrostatic coupling during pulse writing on the ferroelectric film.

To verify our wear reduction analysis, we performed wear tests in which a nominal force $F_N = 7.5$ nN is applied on PtIr probe tips sliding at a velocity of 5 mm/s on an atomically smooth PZT film with a 0.17 nm rms roughness. The tests were carried out in a fluid cell where humidity is precisely controlled from 0 to 80% relative humidity (RH) (see Methods Section). In order to avoid errors due to tip radius variation across experiments, only PtIr-coated silicon probe tips possessing an initial 20 ± 3 nm radius were used (Figure 3a). The PtIr coating was 30 nm thick deposited on a 10 nm adhesive chromium layer. From our analysis, the onset of the adhesive plastic wear regime occurs at $F_N = 60$ nN (42 nN with adhesion effects) (see Methods Section). Therefore, we expect the elastic wear to be the dominant wear mechanism during sliding at 7.5 nN. At 25% RH, a 0.2 nm thick water film would form as determined by ellipsometry, which is about one monolayer and is in agreement with theoretical estimations of the film thickness.²⁷ At this film thickness, it is not energetically favorable for a meniscus to form.²⁶ The nominal 7.5 nN force was modulated sinusoidally at 200 kHz frequency with ± 11 nN force amplitude (see Methods Section). Note that the force amplitude causes the force to be negative during the modulation cycle. However, the tip–sample contact is never lost because the lowest force (-3.5 nN) is much smaller than the adhesion pull-off force between tip–sample measured to be 18 nN for the experimental conditions used (see Supporting Information). This is also confirmed by constantly monitoring the scanning frames during sliding. Note also that the maximum force during the modulation cycle $F_N = 18.5$ nN is below the elastic–plastic transition value of 60 nN.

Figure 3b and c shows scanning electron microscope (SEM) images of the PtIr probe tip after 2.5 and 5 km sliding distances (corresponding to two weeks of continuous sliding) under the conditions mentioned above. The wear volume is estimated from SEM images to be 3.32×10^3 nm³ after 2.5 km and 5.6×10^3 nm³ after 5 km (see Supporting Information for wear volume determination). Figure 3d and e shows a 3×1 matrix of inverted domain dots written by applying 100 μ s wide pulses of 5 V before and after 5 km sliding, with the same domain sizes of 15.6 nm (see Supporting Information for domain size determination). Although the tip has shown a small amount of wear, the write and read resolutions were not lost after 5 km of sliding at 5 mm/s. This is because there are various parameters that determine the inverted domain size in ferroelectric films besides the shape and the size of the probe tip, such as dielectric properties, amplitude of the coercive

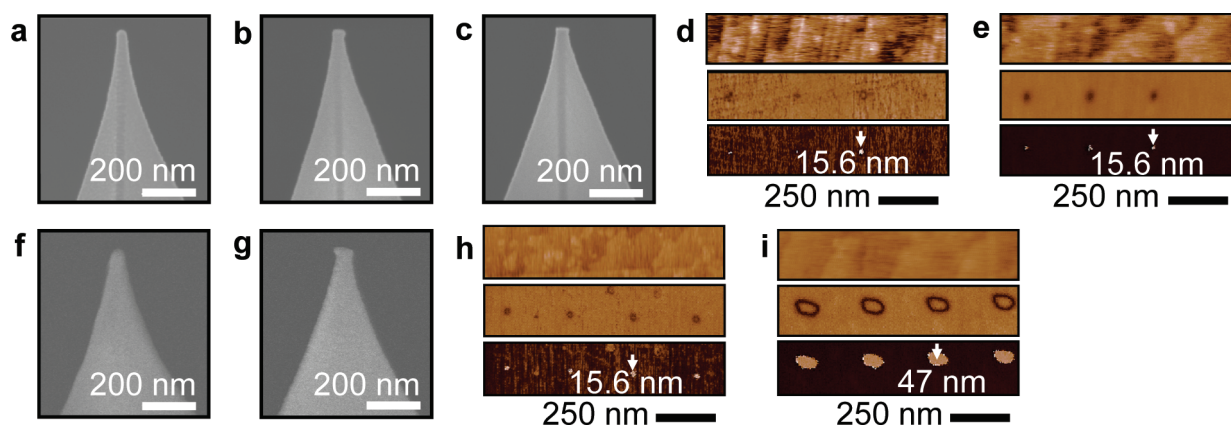


Figure 3. Wear tests on PtIr probe tips sliding over a PZT surface with 0.17 nm rms roughness. (a–c) SEM images of as-received PtIr probe tips prior to sliding (a), after 2.5 (b), and 5 km (c) of sliding at 5 mm/s with an applied normal force $F_N = 7.5$ nN that is modulated at 200 kHz. (d and e) PFM height (top), amplitude (middle), and phase (bottom) images of the PZT–film surface with 3×1 matrix of 15.6 nm inverted domains formed by applying 100 μ s pulses of 5 V using the probe tip prior (d) and after (e) the 5 km sliding experiment. Note that the write and read resolutions did not degrade after the 5 km wear test. (f and g) SEM images of another PtIr probe tip prior (f) and after 500 m (g) of sliding at 5 mm/s with an applied normal force $F_N = 7.5$ nN without force modulation. (h) Height (top), amplitude (middle), and phase (bottom) images of the film surface with 4×1 matrix of 15.6 nm inverted domains formed under the same conditions using the PtIr probe tip prior to the 500 m sliding experiment without modulation. (i) Height (top), amplitude (middle), and phase (bottom) images of the film surface with 4×1 matrix of 47 nm inverted domains formed under the same conditions after the 500 m sliding experiment. The size of the inverted domains increased by 31.2 nm after sliding.

electric field, depolarization, and domain-wall forces (see discussion in Supporting Information). We also performed write and read operations at various stages of the 5 km sliding namely after 1.5, 2.5, and 4 km in which the write and read resolutions were maintained. Note that the write and read conditions were the same as the sliding conditions, *i.e.*, under 7.5 nN force and in the presence of 25% RH, except for the scanning speed which was reduced in order to accurately quantify the change in domain size. Other experiments performed under the same conditions showed no measurable wear from SEM images after 500 m of sliding. Increasing the modulation frequency to 400 kHz also did not show any difference after 500 m sliding, suggesting a negligible frequency effect.

On the other hand, sliding experiments performed without force modulation while keeping other conditions identical, including the 7.5 nN force and the 25% RH level, showed a significant tip blunting after only 500 m sliding with a tip wear volume of 8.2×10^5 nm³ (Figure 3f and g). Figure 3h and i show a 4×1 matrix of inverted domain dots written by applying 100 μ s wide pulses of 5 V before and after the 500 m sliding. Here the dot size increased by 31.4 nm from the as-received tip conditions. Therefore sliding under force modulation within the elastic adhesive wear regime and in the presence of a thin water layer greatly reduces wear. Note that the wear proceeds very smoothly and seems to occur through an atom-by-atom loss process, as previously mentioned. No sudden fracture was observed in any of the experiments, which excludes the presence of any fatigue wear.

Effects of Surface Roughness and Humidity Level. We also investigated the effects of surface roughness and humidity level on wear and write–read resolution. As men-

tioned previously, the roughness of PZT films can be varied by varying deposition parameters, namely the Pb precursor flux¹⁷ (see Methods Section). To obtain tangible wear volumes that are large enough to allow quantitative comparisons of the roughness and the humidity effects over short sliding distances (500 m), accelerated experiments are conducted by increasing the nominal force F_N to 100 nN. Under this force, the onset of the adhesive plastic wear regime, which was estimated previously at 60 nN, is exceeded. The sliding velocity and the force modulation are kept at 5 mm/s and 200 kHz with ± 11 nN force amplitude during the 500 m sliding.

The study of roughness effect was performed by sliding PtIr probe tips over 500 m distance (under 25% RH) on four PZT films possessing an rms roughness of 0.17, 0.23, 0.31, and 0.57 nm, respectively (see Supporting Information for topographic AFM images). These four surfaces are statistically equivalent and are characterized by a Gaussian distribution (see Supporting Information). Figure 4a shows the variation of the inverted domain size and tip wear volume after sliding versus the rms roughness (see Supporting Information for representative PFM and SEM images). Clearly, increasing the rms roughness increases the wear rate considerably and degrades the write–read resolution. The increase in wear rate is due to the fact that the increased roughness initiates the abrasive wear mechanism, which becomes combined to the already existing plastic adhesive wear. The combination of the two mechanisms increases the wear rate considerably even under force modulation and in the presence of a water layer. Therefore, ultrasoft surfaces are required for the proposed wear endurance mechanism to be most efficient in order to eliminate the abrasive wear.

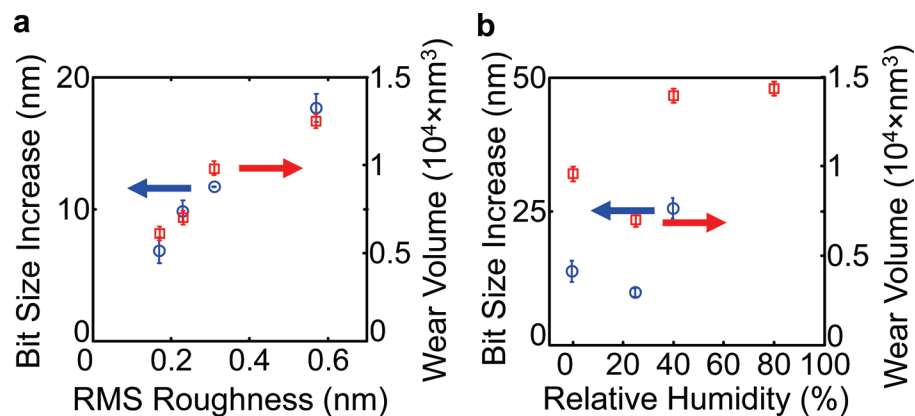


Figure 4. Effects of roughness and RH on bit size and wear volumes. (a) Effect of surface roughness after 500 m of sliding under 25% RH. Four PZT films, possessing respectively an rms roughness of 0.17, 0.23, 0.31, and 0.57 nm, were used. (b) Effect of RH after 500 m of sliding on the PZT film with 0.23 nm rms roughness. All sliding experiments were performed at 5 mm/s with an applied normal force $F_N = 100$ nN that was modulated at 200 kHz. Bit size increase is defined as the difference in bit size before and after sliding. These values are averaged over 16 inverted domains written before and after sliding at pulses ranging from 3 to 8 V, and the error bars correspond to the standard deviation of each set of bit size increase.

The effect of humidity level on the inverted domain size and the tip wear after sliding, is shown in Figure 4b. The experiments were performed on the PZT sample with 0.23 rms surface roughness. Here we see that both bit size and wear volume first decrease after sliding as the RH level is increased from the dry condition, which supports our claim that adding a water layer provides additional stress relaxation during sliding under force modulation. However, as the RH level further increases, the bit size and the wear volume start increasing considerably. This is because at higher RH levels, it becomes energetically favorable for a meniscus to form at the tip–sample interface.²⁶ The stress relaxation mechanism will thus disappear. Instead, such a meniscus will pull the probe tip further into the surface, which causes further tip wear, which is usually observed when RH levels are increased.¹¹

Note also that beyond 40% RH, inverted domains did not retain and disappeared almost immediately after the writing process. This is why bit sizes are only reported for RH below 40%. This is due to the fact that water becomes abundant at the tip–sample interface to the point where electric field distribution underneath the probe tip is changed, which affects the pulse writing process. Moreover, as the probe tip passes over written bits during reading, the water meniscus bridges neighboring domains, resulting in charge neutralization and bit destabilization. The results also show that the force modulation alone can moderately reduce the tip wear under dry conditions. As discussed previously, this is due to the stress relief on atomic bonds involved in the wear process during a modulation cycle. This reduction of wear, however, is not as significant as in the presence of a thin water film. Therefore, for the wear endurance mechanism to be most efficient, ideal sliding has to occur under very low forces, with force modulation, on ultrasoft surfaces, and in the presence of thin water films under optimized humidity.

The current wear endurance mechanism was demonstrated on PtIr-coated probes, which possess about the same hardness and elastic modulus as the ferroelectric films, as previously discussed. We believe that the modulation mechanism in the presence of a thin water film can further be enhanced by the use of ultrahard and more importantly ultrastiff conductive tip coatings. Such coatings have to be smooth and be deposited at low temperatures. Perhaps the use of boride-based metals, such as HfB_2 , which possess hardness and elastic modulus in the range of 40–400 GPa, can provide such an enhancement.²⁸ Such coatings can be deposited using low-temperature chemical vapor deposition at around 200 °C and possess 1–3 nm surface roughness.²⁸

Final Note. Note that during the preparation of this manuscript we became aware of a related study with similar findings from Lantz *et al.*²⁹ In this study, force modulation is shown to improve tip-wear endurance in silicon tips sliding on a polyaryletherketone polymeric surface after 750 m of sliding at 1.5 mm/s and under dry (vacuum) conditions. The authors attribute the wear endurance mechanism to a friction reduction during force modulation by performing friction experiments at a much lower velocity (100 nm/s and 1 $\mu\text{m/s}$) and under ambient conditions, which were previously demonstrated by several previous studies.^{19–23} At such low velocities the stick–slip mechanism has an important role which is eliminated by force modulation.^{19,23} On the other hand, at the reported sliding velocity of 1.5 mm/s at which the wear experiments were performed, the stick–slip behavior is not relevant given the relatively high speed, and it is not obvious that friction reduction during force modulation alone is the cause of the wear endurance. We suspect that the force modulation is only one of the key factors that reduced the tip wear. We think the much higher hardness and elastic modulus of silicon compared to the polyaryletherke-

tone polymeric surface, the low applied force, and the low surface roughness also contributed to the reported low wear of silicon tips. Moreover, the reported applied velocity and sliding distance are much lower than actual device operational conditions.

In contrast to this previous paper, we systematically studied multifactors including force modulation, force load, surface roughness, and thin water-layer lubrication, which all critically contribute to the tip wear, under the sliding velocity and the distance that are comparable to actual operational conditions of probe-based storage devices. We demonstrated that excellent tip-wear endurance is attainable if all conditions are systematically controlled despite the fact that our Ptlr-coated tips and the PZT films possess similar mechanical properties (hardness and elastic modulus).

CONCLUSIONS

In summary, we have developed a wear endurance mechanism which allows a conductive Ptlr-coated probe tip sliding over a ferroelectric film at a 5 mm/s velocity to retain its write–read resolution over a 5 km

distance, which corresponds to a 5 year device life-time. This mechanism is achieved by sliding the probe tip at low applied forces on atomically smooth surfaces with force modulation and in the presence of thin water films under optimized humidity. Under the conditions of low applied forces on atomically smooth surfaces, the adhesive elastic wear regime is dominant, and the wear rate is decreased by orders of magnitude. In this regime, the wear volume is inversely dependent on the elastic modulus of the coating rather than its hardness. Modulating the force in the presence of a thin water layer, which acts as a viscoelastic film, further reduces the wear volume to insignificant amounts. Our results could lead to parallel probe-based data storage devices that exceed the capabilities of current hard drive and solid-state disks given the ultrahigh density capabilities demonstrated here (3.6 Tbit/inch²). It can also allow other scanning probe-based systems, such as atomic force microscope (AFM)-based lithography^{15,16} to be competitive with the current state-of-the-art optical and electron-beam lithography systems.

METHODS

PZT Ferroelectric Film Growth. Single crystal PZT films are deposited on single crystal SrRuO₃ (SRO, 50 nm thick)/SrTiO₃(100) substrates using metal–organic chemical vapor deposition (MOCVD) at a 605 °C temperature under a 5 Torr pressure with Ti and Zr precursor fluxes of 0.07 and 0.025 mL/min. The Pb self-regulation flux window is from 0.11 to 0.21 mL/min. By increasing the Pb flux, the film rms roughness first decreases rapidly to reach a minimum value at a Pb flux of 0.165 mL/min. At 0.165 mL/min, the rms roughness is 0.17–0.20 nm, which corresponds to atomically smooth films. It then increases rapidly again to a maximum value of 0.60 nm. (See ref 17.)

Data Write/Read. The write/read experiments were performed using Asylum Research MFP-3D and Veeco Dimension 3100 scanning probe microscopes. The Ptlr-coated probe tips are used as conducting probes to write inverted domain dots on the PZT film. To avoid errors due to tip radius variation across experiments, only as-received Ptlr-coated probe tips possessing an initial 20 nm radius are used. The probe tips used were made from silicon. The Ptlr coating was 30 nm deposited on a 10 nm Cr intermediate adhesive layer. The ferroelectric PZT film is initially polarized in an upward direction. A Ptlr probe is first brought into contact with the film surface. Positive (or negative for erasing) electrical pulses varying from 3 to 10 V with a pulse width varying from 500 ns to 100 μs are then applied to the PZT surface through the conductive Ptlr probe. The ferroelectric domains are imaged using piezoresponse-force microscopy (PFM), where domain walls show dark contrast in amplitude images, and the inverted domains show 180° phase shift to the background film.

All experiments are carried out within a fluid cell which allows for full environmental control. High-purity nitrogen can be fed through to keep a clean environment within the cell in order to avoid carbonaceous contamination on the probe tip and the PZT sample. Water vapor from a high-purity water container can also be fed through with RH precisely controlled from 0 to 80%.

Wear/Sliding Experiments. Wear experiments were performed by scanning the probe tip over two 80 μm lines with a 5 mm/s velocity under either contact or PFM mode with image data acquisition enabled to monitor probe tip contact and cantilever deflection during sliding. The probe tip was scanned parallel to the leveled surface. The scan was driven with a sinusoidal wave-

form to prevent scanner ringing, which would occur when a triangular waveform is used.

Force modulation is obtained by performing the sliding under PFM mode which operates at the cantilever resonant frequency and superimposes an AC field over the constant force mode. Experiments were carried out at the second and third PFM frequency peaks, which correspond to 200 and 400 kHz, respectively, with ±10 kHz variation from cantilever to another. The modulation amplitude was determined by monitoring the deflection during sliding, which was equal to 0.15 ± 0.22 V with a set point of 0.15 V. This corresponds to a force of 7.5 ± 11 nN. The same force amplitude was obtained when 100 nN forces were applied. Bit writing before and after sliding is performed under the same force and humidity conditions as during sliding. Moreover, to avoid errors due to tip radius variation across experiments, only as-received Ptlr-coated probe tips possessing an initial 20 nm radius are used. Note that we have tried negative and zero mean loads. However, the tip–sample contact was lost after usually 0.5–1 km of sliding as the lowest force (–11 nN for 0 nominal force) was getting closer to the adhesion pull-off force between tip–sample that we estimated under static conditions to be 17.82 nN for the humidity conditions used (see section below). The loss of contact could be due to a lowering of the pull-off force, which, under sliding conditions, can be reduced by the effects of shear forces.

Determination of Minimum Transition Force from Elastic-to-Plastic Adhesive Wear. Assuming a Hertzian contact between the Ptlr probe tip and the PZT film, the mean flow pressure is $p_m = F_N / \pi a^2$, where F_N is the applied normal force, and a is the contact radius and is equal to $a = (3F_N R / 4E^*)^{1/3}$. E^* is the composite elastic modulus between the Ptlr coating and the PZT films, which is defined as $1/E^* = (1 - \nu_{Ptlr}^2)/E_{Ptlr} + (1 - \nu_{PZT}^2)/E_{PZT}$, where E_{Ptlr} and E_{PZT} are the elastic moduli of Ptlr and PZT and are taken to be equal to 190 and 123 GPa, respectively, as determined by nanoindentation; ν_{Ptlr} and ν_{PZT} are the Poisson's ratio of Ptlr and PZT and are both taken to be equal to 0.3. Under sliding, the transition from elastic to plastic adhesive wear regimes occurs when the mean flow pressure p_m reaches the value $H/(1 + 9\mu^2)^{1/2}$, where H is the hardness, and μ is the friction coefficient (see ref 18). The hardness of Ptlr is $H = 7$ GPa as determined from nanoindentation, and the friction coefficient is estimated to be 0.5. Under these conditions, the mean pressure p_m reaches the

value $H/(1 + 9 \mu^2)^{1/2}$ when a normal force $F_N = 60$ nN is applied. Note that the Hertzian contact does not include the effect of adhesion and therefore underestimates the contact area. For the current contact, *i.e.*, stiff materials, small contacts, and long-range adhesion forces, the Derjaguin–Muller–Toporov (DMT) adhesion model can be used. In this model the contact radius is equal to $a = ((3R/4E^*)(F_N + 2\pi\gamma R))^{1/3}$. The additional term $2\pi\gamma R$ represents the adhesion pull-off term (see ref 10), where γ is the energy of adhesion. Given that contact occurs in the presence of a thin water layer, the adhesion energy can be assumed to be that of water which is equal to $\gamma = 140$ mN/m. In this case, the onset of the adhesive plastic wear regime is estimated to occur at $F_N \cong 42$ nN.

Acknowledgment. Part of Y.Z.'s work was supported by the Office of Science, Office of Basic Energy Sciences, of the United States Department of Energy under contract no. DE-AC02-05CH11231.

Supporting Information Available: Procedure of ultrahigh density writing. Mapping of electrical hot spots. Adhesion pull-off force determination under 25% RH. Determination of wear volume. Domain size determination. Effect of probe shape on write–read resolution. Carbonaceous contamination from organic films. Effect of roughness and RH on bit size and wear volumes. This material is available free of charge *via* the Internet at <http://pubs.acs.org>.

REFERENCES AND NOTES

- Ahn, C. H.; Tybell, T.; Antognazza, L.; Char, K.; Hammond, R. H.; Beasley, M. R.; Fischer, Ø.; Triscone, J.-M. Nonvolatile Electronic Writing of Epitaxial $\text{Pb}(\text{Zr}_{0.52}\text{Ti}_{0.48})\text{O}_3/\text{SrRuO}_3$ Heterostructures. *Science* **1997**, *276*, 1100–1103.
- Heck, J.; Adams, D.; Belov, N.; Chou, T. A.; Kim, B.; Kornelsen, K.; Ma, Q.; Rao, V.; Severi, S.; Spicer, D.; et al. Ultra-High Density MEMS Probe Memory Device. *Microelectron. Eng.* **2010**, *87*, 1198–1203.
- Cho, Y.; Hashimoto, S.; Odagawa, N.; Tanaka, K.; Hiranaga, Y. Realization of 10 Tbit/in² Memory Density and Subnanosecond Domain Switching Time in Ferroelectric Data Storage. *Appl. Phys. Lett.* **2005**, *87*, 232907.
- Ahn, C. H.; Rabe, M. R.; Triscone, J.-M. Ferroelectricity at the Nanoscale: Local Polarization in Oxide Thin Films and Heterostructures. *Science* **2004**, *303*, 488–491.
- Cho, Y.; Hashimoto, S.; Odagawa, N.; Tanaka, K.; Hiranaga, Y. Nanodomain Manipulation for Ultrahigh Density Ferroelectric Data Storage. *Nanotechnol.* **2006**, *17*, S137–S141.
- Vettiger, P.; Cross, G.; Despont, M.; Drechsler, U.; Dürig, U.; Gotsmann, B.; Häberle, W.; Lantz, M. A.; Rothuizen, H. E.; Stutz, R.; et al. The 'Millipede' - Nanotechnology Entering Data Storage. *IEEE Trans. Nanotechnol.* **2002**, *1*, 39–55.
- Pantazi, A.; Sebastian, A.; Antonakopoulos, T. A.; Bächtold, P.; Bonaccio, A. R.; Bonan, J.; Cherubini, G.; Despont, M.; DiPietro, R. A.; Drechsler, U.; et al. E. Probe-Based Ultrahigh-Density Storage Technology. *IBM J. Res. Dev.* **2008**, *52*, 493–511.
- Hamann, H.; O'Boyle, M.; Martin, Y. C.; Rooks, M.; Wickramasinghe, H. K. Ultra-High-Density Phase-Change Storage and Memory. *Nat. Mater.* **2006**, *5*, 383–387.
- Forrester, M. G.; Ahner, J. W.; Bedillion, M. D.; Bedoya, C.; Bolten, D. G.; Chang, K.-C.; de Gersem, G.; Hu, S.; Johns, E. C.; Nassirou, M.; et al. Charge-Based Scanning Probe Readback of Nanometer-Scale Ferroelectric Domain Patterns at Megahertz Rates. *Nanotechnol.* **2009**, *20*, 225501.
- Knoll, A.; Bächtold, P.; Bonan, J.; Cherubini, G.; Despont, M.; Drechsler, U.; Dürig, U.; Gotsmann, B.; Häberle, W.; Hagleitner, C.; et al. Integrating Nanotechnology into a Working Storage Device. *Microelectron. Eng.* **2006**, *83*, 1692–1697.
- Bhushan, B.; Kwak, K. J.; Palacio, M. Nanotribology and Nanomechanics of AFM Probe-Based Data Recording Technology. *J. Phys.: Condens. Matter* **2008**, *20*, 365207.
- Gotsmann, B.; Lantz, M. A. Atomistic Wear in a Single Asperity Sliding Contact. *Phys. Rev. Lett.* **2008**, *101*, 125501.
- Lantz, M. A.; Gotsmann, B.; Dürig, U. T.; Vettiger, P.; Nakayama, Y.; Shimizu, T.; Tokumoto, H. Carbon Nanotube Tips for Thermomechanical Data Storage. *Appl. Phys. Lett.* **2003**, *83*, 1266–1268.
- Tayebi, N.; Yoshie, N.; Chen, R. C.; Collier, P. C.; Giapis, K. P.; Zhang, Y. Nanopencil as a Wear-Tolerant Probe for Ultrahigh Density Data Storage. *Appl. Phys. Lett.* **2008**, *93*, 103112.
- Tseng, A. A.; Notagiaco, A.; Chen, T. P. Nanofabrication by Scanning Probe Microscope Lithography: a Review. *J. Vac. Sci. Technol., B: Microelectron. Nanometer Struct.—Process., Meas., Phenom.* **2005**, *23*, 877–894.
- Salaite, K. S.; Wang, Y.; Mirkin, C. A. Applications of Dip-Pen Nanolithography. *Nat. Nanotechnol.* **2007**, *2*, 145–155.
- Chen, Z.; Tran, Q.; Franklin, N.; Chen, R.; Wang, L.-P.; Ma, Q.; Rao, V. R. Growth Sub-Window for Epitaxially Synthesizing Atomically-Smooth High-Polarization $\text{Pb}(\text{Zr}, \text{Ti})\text{O}_3$ Single Crystal Films for Tb/inch² Scanning Probe Memory Applications. *Appl. Phys. Lett.*; manuscript in preparation.
- Bhushan, B. *Introduction to Tribology*; Wiley: New York, 2002.
- Socoliuc, A.; Bennewitz, R.; Gnecco, E.; Meyer, E. Transition From Stick-Slip to Continuous Sliding in Atomic Friction: Entering a New Regime of Ultralow Friction. *Phys. Rev. Lett.* **2004**, *92*, 134301.
- Dinelli, F.; Biswas, S. K.; Briggs, G. A. D.; Kolosov, O. V. Ultrasound Induced Lubricity in Microscopic Contact. *Appl. Phys. Lett.* **1997**, *71*, 1177–1179.
- Behme, G.; Hesjedal, T. Influence of Surface Acoustic Waves on Lateral Forces in Scanning Force Microscopies. *J. Appl. Phys.* **2001**, *89*, 4850–4856.
- Socoliuc, A.; Gnecco, E.; Maier, S.; Pfeiffer, O.; Baratoff, A.; Bennewitz, R.; Meyer, E. Atomic-Scale Control of Friction by Actuation of Nanometersized Contacts. *Science* **2006**, *313*, 207–210.
- Gnecco, E.; Socoliuc, A.; Maier, S.; Gessler, J.; Glatzel, T.; Baratoff, A.; Meyer, E. Dynamic Superlubricity on Insulating and Conductive Surfaces in Ultra-High Vacuum and Ambient Environment. *Nanotechnol.* **2009**, *20*, 025501.
- Kopta, S.; Salmeron, M. The Atomic Scale Origin of Wear on Mica and its Contribution to Friction. *J. Chem. Phys.* **2000**, *113*, 8249–8252.
- Mo, Y.; Turner, K. T.; Szulfarska, I. Friction Laws at the Nanoscale. *Nature* **2009**, *457*, 1116–1119.
- Israelachvili, J. N. *Intermolecular and Surface Forces*; Academic Press: Maryland Heights, MO, 1991.
- Colchero, J.; Storch, A.; Luna, M.; Gomez-Herrero, J.; Baro, A. M. Observation of Liquid Neck Formation with Scanning Force Microscopy Techniques. *Langmuir* **1998**, *14*, 2230–2234.
- Jayaraman, S.; Gerbi, J. E.; Yang, Y.; Kim, D. Y.; Chatterjee, A.; Bellon, P.; Girolami, G. S.; Chevalier, J. P.; Abelson, J. R. HfB₂ and Hf-B-N Hard Coatings by Chemical Vapor Deposition. *Surf. Coat. Technol.* **2006**, *200*, 6629–6633.
- Lantz, M. A.; Wiesmann, D.; Gotsmann, B. Dynamic Superlubricity and the Elimination of Wear on the Nanoscale. *Nat. Nanotechnol.* **2009**, *4*, 586–592.